Regular Article

Radioiodinated Peptidic Imaging Probes for *in Vivo* Detection of Membrane Type-1 Matrix Metalloproteinase in Cancers

Naoya Kondo,[a] Takashi Temma,[a,b] Yoichi Shimizu,[a] Masahiro Ono,[a] and Hideo Saji*[,a]

[a] *Department of Patho-Functional Bioanalysis, Graduate School of Pharmaceutical Sciences, Kyoto University; 46–29 Yoshida Shimoadachi-cho, Sakyo-ku, Kyoto 606–8501, Japan: and* [b] *Department of Investigative Radiology, National Cerebral and Cardiovascular Center Research Institute; 5–7–1 Fujishiro-dai, Suita, Osaka 565–8565, Japan.*
Received April 9, 2015; accepted June 10, 2015

Membrane type-1 matrix metalloproteinase (MT1-MMP) plays pivotal roles in tumor progression and metastasis, and holds great promise as an early biomarker for malignant tumors. Therefore, the ability to evaluate MT1-MMP expression could be valuable for molecular biological and clinical studies. For this purpose, we aimed to develop short peptide-based nuclear probes because of their facile radiosynthesis, chemically uniform structures, and high specific activity, as compared to antibody-based probes, which could allow them to be more effective for *in vivo* MT1-MMP imaging. To the best of our knowledge, there have been no reports of radiolabeled peptide probes for the detection of MT1-MMP in cancer tissues. In this study, we designed and prepared four probes which consist of a MT1-MMP-specific binding peptide sequence (consisting of L or D amino acid isomers) and an additional cysteine (at the N or C-terminus) for conjugation with *N*-(*m*-[$^{123/125}$I]iodophenyl) maleimide. We investigated probe affinity, probe stability in mice plasma, and probe biodistribution in tumor-bearing mice. Finally, *in vivo* micro single photon emission computed tomography (SPECT) imaging and *ex vivo* autoradiography were performed. Consequently, [^{123}I]I-DC, a D-form peptide probe radioiodinated at the C-terminus, demonstrated greater than 1000-fold higher specific activity than previously reported antibody probes, and revealed comparably moderate binding affinity. [^{125}I]I-DC showed higher stability as expected, and [^{123}I]I-DC successfully identified MT1-MMP expressing tumor tissue by SPECT imaging. Furthermore, *ex vivo* autoradiographic analysis revealed that the radioactivity distribution profiles corresponded to MT1-MMP-positive areas. These findings suggest that [^{123}I]I-DC is a promising peptide probe for the *in vivo* detection of MT1-MMP in cancers.

Key words membrane type-1 matrix metalloproteinase (MT1-MMP); peptide; *in vivo* imaging

Metastasis is the most frequent cause of death in cancer patients.[1] In order to metastasize, tumor cells must break through the basement membrane and invade dense networks of the interstitial extracellular matrix (ECM) that surrounds cancer cells.[2] Matrix metalloproteinases (MMPs) are a family of zinc-dependent proteases responsible for degrading various ECM components. While most MMPs are secreted as soluble zymogens, a subfamily of membrane-type MMPs (MT-MMPs) is expressed on the cell membrane and mediate pericellular proteolysis.[3,4] Among MT-MMPs, MT1-MMP is the most prominent member and is the major pericellular protease involved in degrading triple helical collagen type I.[5] In addition, MT1-MMP activates MMP zymogens such as proMMP-2 and proMMP-13, which are also significantly involved in tumor cell invasion and metastasis.[6,7] As MT1-MMP is closely associated with tumor malignancy and holds great promise as an early biomarker of malignant tumors,[8,9] *in vivo* monitoring of MT1-MMP expression could provide meaningful data for molecular biology and clinical studies.

Since nuclear medical techniques are optimal for non-invasive quantitative evaluation of biological molecules deep within the body, we recently developed ^{99m}Tc-labeled anti-MT1-MMP monoclonal immunoglobulin G (IgG)[10] and ^{111}In-labeled miniaturized antibodies (scFv and diabody)[11] as radiolabeled probes for nuclear medical imaging of MT1-MMP. Although these probes could be used for imaging MT1-MMP in cancer, antibody derivatives have several undesirable characteristics when used as molecular imaging probes. In addition to the high cost of producing antibody derivatives,[12] radiolabeling of these antibodies could generate heterogeneous mixtures because a radioisotope can non-selectively react with several amino acid residues in a protein sequence depending on the radioisotope introduction reagent.[13] Moreover, radiolabeled high molecular weight probes may show low apparent specific radioactivity (radioactivity per gram) because precursors remaining after the radiolabeling reaction cannot be separated by ordinary size exclusion HPLC methods.[11] The presence of substantial amounts of precursor could inhibit the accumulation of a radiolabeled probe in tumors and complicate *in vivo* imaging. On the basis of these considerations, we hypothesized that low molecular weight probes, such as those having a short peptide core, could overcome these drawbacks. To the best of our knowledge, there have been no reports on radiolabeled peptide probes for the detection of MT1-MMP in cancers. Thus, we aimed to develop radiolabeled peptide probes to detect MT1-MMP.

To develop these radiolabeled peptide probes, we selected a MT1-MMP binding peptide (HWKHLHNTKTFL) that was recently discovered by phage display technology[14] to serve as the core structure of the molecular probe. We then added a Cys residue at the N- or C-terminus of the peptide (LN and LC) to allow facile radiolabeling of the thiol group by *N*-(*m*-[$^{123/125}$I]iodophenyl)maleimide ([$^{123/125}$I]IPM). We also designed probes with D-amino acids (DN and DC) in order to improve the *in vivo* stability.[15] In this study we synthesized four radioiodinated peptidic probes and evaluated *in vitro*, *ex vivo* and *in vivo* effectiveness of the probes to image MT1-MMP in cancers.

* To whom correspondence should be addressed. e-mail: hsaji@pharm.kyoto-u.ac.jp

MATERIALS AND METHODS

Preparation of Peptides All reagents were purchased from Watanabe Chemical Industries, Ltd. (Hiroshima, Japan) unless otherwise noted. The peptide sequences CGHWKHLHNTKTFL-NH_2 (LN and DN) and HWKHLHNTKTFLC-NH_2 (LC and DC) were synthesized with either L-amino acids or D-amino acids using Fmoc solid phase methodology and acetylation of the amino group at the N-terminus followed by cleavage from the resin with trifluoroacetic acid (TFA)–water (19 : 1). The products were purified on a reverse phase (RP)-HPLC system (Shimadzu Corporation, Kyoto, Japan) equipped with a C18-reverse phase column (COSMOSIL 5C18-AR-II 10 i.d.×250 mm; Nacalai Tesque, Inc., Kyoto, Japan). The mobile phase was a linear gradient with solvent A (0.1% TFA in water) and solvent B (0.1% TFA in acetonitrile) increasing from 10% solvent B to 70% solvent B over 30 min at a flow rate of 2.5 mL/min (these conditions were used for all experiments in this study). Peptides were characterized by analytical HPLC performed using the same conditions as the semi-preparative HPLC and by matrix assisted laser desorption/ionization mass spectrometry (AXIMA-CFR Plus; Shimadzu Corporation).

Radiolabeling Na[^{125}I]I was purchased from MP Biomedicals, Inc. (Santa Ana, CA, U.S.A.). NH_4[^{123}I]I was kindly supplied by Nihon Medi-Physics Co., Ltd. (Tokyo, Japan). [$^{123/125}$I]IPM and non-radioactive IPM were prepared according to previously described procedures.[16] LN (100 μg) was dissolved in phosphate buffered saline (PBS)(−), and the solution was added to the ([$^{123/125}$I]IPM) solution. After incubation for 30 min at rt, the reaction product ([$^{123/125}$I]I-LN) was purified by RP-HPLC and the purified product was analyzed again by RP-HPLC to measure the radiochemical purity. Nonradioactive I-LN was obtained by reacting LN with non-radioactive IPM. LC, DN and DC were also radiolabelled with [$^{123/125}$I]IPM in the same manner.

***In Vitro* Binding Assay** For construction of the MT1-MMP fusion protein, a cDNA clone of human MT1-MMP (FXC01469) was obtained from the Kazusa DNA Research Institute and was cloned into the pFC30A His6HaloTag T7 Flexi Vector (Promega Corporation, Tokyo, Japan). The vector was added to KRX competent cells (Promega Corporation) and heat-shock transformation was conducted. After transformation, the His-tagged MT1-MMP protein was expressed and purified using Ni-NTA magnetic beads (QIAGEN, Tokyo, Japan). The MT1-MMP protein was immobilized on 200 μL of Ni-NTA magnetic beads by incubation for 1 h at rt, and the beads were then washed with wash buffer (50 mM NaH_2PO_4, 300 mM NaCl, 10 mM imidazole, 0.05% Tween 20, pH 8.0).

[^{125}I]I-LN (185 kBq) was added to I-LN (1.6×10^{-9} mol) and after a two-fold serial dilution the mixture was added to 5 μL of prepared beads, which were then incubated for 90 min at rt. A blocking group was prepared and added in excess (2×10^{-6} mol) of I-LN to evaluate non-specific binding to the protein. After washing three times, [^{125}I]I-LN bound to MT1-MMP was eluted with elution buffer (50 mM NaH_2PO_4, 300 mM NaCl, 250 mM imidazole, 0.05% Tween 20, pH 8.0), and the radioactivity was counted with a NaI well-type scintillation counter (1470 WIZARD; PerkinElmer, Inc., Kanagawa, Japan). Values for the dissociation constants (K_D) were determined from saturation curves of three independent experiments using GraphPad Prism 5.0. The K_D values of [^{125}I]I-LC, [^{125}I]I-DN and [^{125}I]I-DC were determined in the same manner.

I-LN (2×10^{-13}–2×10^{-8} mol) was added to 5 μL of the beads, [^{125}I]I-LN (3.7 kBq) was then added, and the mixture was incubated for 90 min at rt. After washing three times, [^{125}I]I-LN bound to MT1-MMP was eluted with elution buffer, and the radioactivity was counted using a NaI well-type scintillation counter. Values for the half-maximal inhibitory concentration (IC_{50}) were determined from displacement curves of three independent experiments using GraphPad Prism 5.0. The IC_{50} values of I-LC, I-DN and I-DC were also evaluated in the same manner.

Stability Assay in Plasma Plasma was obtained from the blood of male ddY mice (7-13 weeks old, Japan SLC, Hamamatsu, Japan) by centrifugation at 2500×***g*** for 10 min. Plasma (100 μL) and [^{125}I]I-LN, [^{125}I]I-LC, [^{125}I]I-DN or [^{125}I]I-DC (740 kBq) were incubated for 30, 60, or 120 min at 37°C, and reactions were stopped by the addition of acetonitrile to each sample. The samples were centrifuged at 2500×***g*** for 10 min. The supernatants were then filtered with a syringe filter (Millex-LH, Millipore). After filtration, the samples were analyzed and fractionated by RP-HPLC (30 s×60 fractions) followed by radioactivity counting with a scintillation counter.

Preparation of Tumor-Bearing Mice Female BALB/c *nu-nu* mice (5 weeks old, Japan SLC, Hamamatsu, Japan) were housed under a 12 h light/12 h dark cycle and given free access to food and water. Animal experiments were conducted in accordance with institutional guidelines and approved by the Kyoto University Animal Care Committee. Human fibrosarcoma cell line (HT1080, ATCC, Manassas, VA, U.S.A.), which are known to highly express MT1-MMP were suspended in PBS(−) followed by subcutaneous inoculation into the right hind legs of BALB/c mice (5×10^6 cells/100 μL) for the *in vivo* biodistribution study as well as *ex vivo* autoradiography and immunohistochemistry. For single photon emission computed tomography (SPECT)/CT imaging, cells were inoculated into the left shoulder of the mouse.

***In Vivo* Biodistribution Study** Animals were divided into groups (n=3–4) for time point studies with an approximately equal distribution of tumor sizes on the day before the study. Animals were fasted for 6 h before administration of the radiopharmaceutical. The mice were sacrificed 2, 10, 30, 60, and 120 min after intravenous administration of [^{125}I]I-LN, [^{125}I]I-LC, [^{125}I]I-DN or [^{125}I]I-DC (37 kBq/100 μL saline). Blood, heart, lungs, liver, kidneys, stomach, intestine, spleen, pancreas, muscle, and tumor tissues were excised, weighed and counted for radioactivity.

SPECT/CT Imaging [^{123}I]I-DC (33.3 MBq/100 μL saline) was injected into a HT1080 tumor-bearing mouse. The mouse was sacrificed by anesthesia overdose 30 min after probe injection. SPECT and CT images with the thoracic region as the field of view were obtained using the U-SPECT-II/CT system (MILabs, Utrecht, the Netherlands) with 0.6 mm pinhole collimators (SPECT conditions, 30 min×1 frame; CT conditions, accurate full angle mode in 65 kV/615 μA). SPECT images were reconstructed by the OSEM method (16 subsets, 6 iterations) with a 0.4 mm Gaussian filter.

***Ex Vivo* Autoradiography and Immunohistochemistry** A tumor-bearing mouse was sacrificed 30 min after intravenous administration of [^{123}I]I-DC (33.3 MBq/100 μL saline).

The tumor was removed and immediately frozen. After freezing, 10 μm thick sections of the tumor were prepared with a cryomicrotome (CM1900; Leica Microsystems, Tokyo, Japan) and exposed to imaging plates (BAS-SR; FUJI PHOTO FILM, Tokyo, Japan) for 6 h. Autoradiograms of these sections were obtained with a BAS5000 scanner (FUJI PHOTO FILM). The adjacent sections were blocked with 1% BSA and incubated overnight at 4°C with a primary monoclonal antibody to MT1-MMP (F-84, Daiichi Fine Chemical Co., Ltd., Toyama, Japan). After rinsing with PBS(−) containing 0.1% Tween20, sections were reacted with Alexa Fluor 647 goat anti-mouse IgG (H+L) antibody (Molecular Probes, Eugene, OR, U.S.A.) for 1 h at rt. Fluorescence images were then acquired by fluorescence microscopy (BIOREVO BZ9000, Keyence Japan Co., Osaka, Japan) using the following filters: excitation wavelength, 590 to 650 nm; emission wavelength, 663 to 737 nm. Fluorescence images were analyzed with BZ-II Analyzer 1.10 software (Keyence Japan Co.).

Statistics Data are presented as means±standard deviation (S.D.). A two-way ANOVA followed by *post-hoc* Bonferroni test was used to evaluate the significance of differences. Differences at a 95% confidence level ($p<0.05$) were considered significant.

RESULTS

Radiolabeling The probes evaluated in this study are shown in Table 1 and Fig. 1. The radiochemical yields of [^{125}I]I-LN, [^{125}I]I-LC, [^{125}I]I-DN and [^{125}I]I-DC from [^{125}I]IPM were 77.5, 79.3, 76.3 and 77.2%, respectively. The radiochemical purities of these probes were above 99% after RP-HPLC purification. Moreover, HPLC traces indicated that the radiolabeled probes were successfully separated from unreacted precursor peptides (Fig. 2a). The specific radioactivities of these probes were estimated to be above 88.8 MBq/μg, while [^{123}I]I-DC for SPECT imaging was also successfully synthesized at a radiochemical yield of 70.2%, radiochemical purity above 99%, and a specific radioactivity estimated to be above 260 MBq/μg.

***In Vitro* Binding Assay** The binding affinity of each probe to the MT1-MMP protein was evaluated by an *in vitro* binding saturation assay. Saturation curves revealed K_D

Table 1. Probes Evaluated in This Study

Name	Amino acid sequence	MS	IC_{50} (μM)	K_D (μM)
I-LN	Ac-C(IPM)GHWKHLHNTKTFL	$C_{91}H_{125}IN_{26}O_{20}S$ *m/z* Calcd: 2060.83 Found: 2061.59 $(M+H)^+$	1.43±0.47	0.71±0.44
I-LC	Ac-HWKHLHNTKTFLC(IPM)	$C_{89}H_{122}IN_{25}O_{19}S$ *m/z* Calcd: 2003.81 Found: 2004.84 $(M+H)^+$	0.52±0.04	0.42±0.13
I-DN	Ac-c(IPM)Ghwkhlhnktfl	$C_{91}H_{125}IN_{26}O_{20}S$ *m/z* Calcd: 2060.83 Found: 2061.77 $(M+H)^+$	1.76±0.52	0.97±0.25
I-DC	Ac-hwkhlhnktflc(IPM)	$C_{89}H_{122}IN_{25}O_{19}S$ *m/z* Calcd: 2003.81 Found: 2004.85 $(M+H)^+$	1.02±0.14	0.87±0.19

Lower case letters designate D-amino acids. IPM, *N*-(*m*-iodophenyl)maleimide.

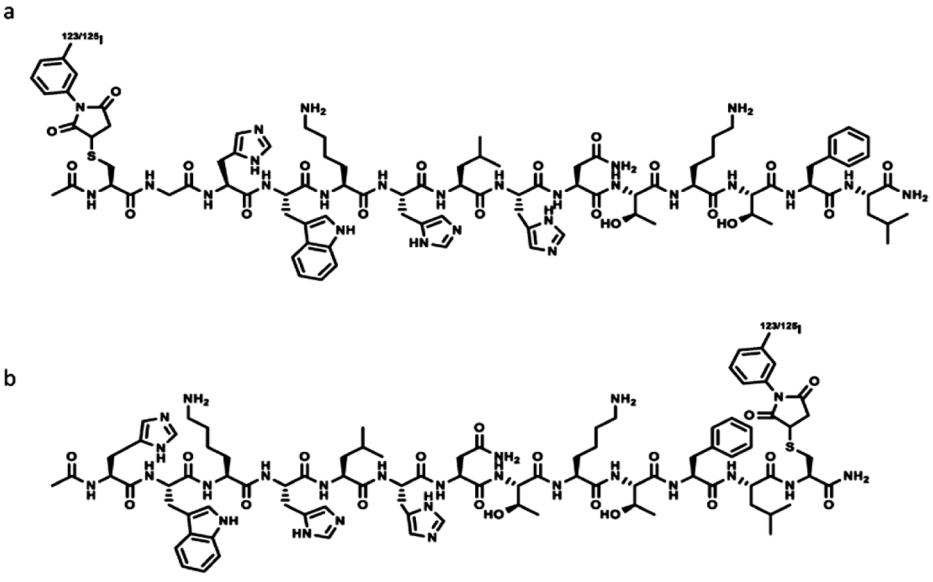

Fig. 1. Structures of Newly Developed Radioiodinated Probes in This Study

(a) [$^{123/125}$I]I-LN; (Ac-C(IPM)GHWKHLHNTKTFL) and (b) [$^{123/125}$I]I-LC; (Ac-HWKHLHNTKTFLC(IPM)).

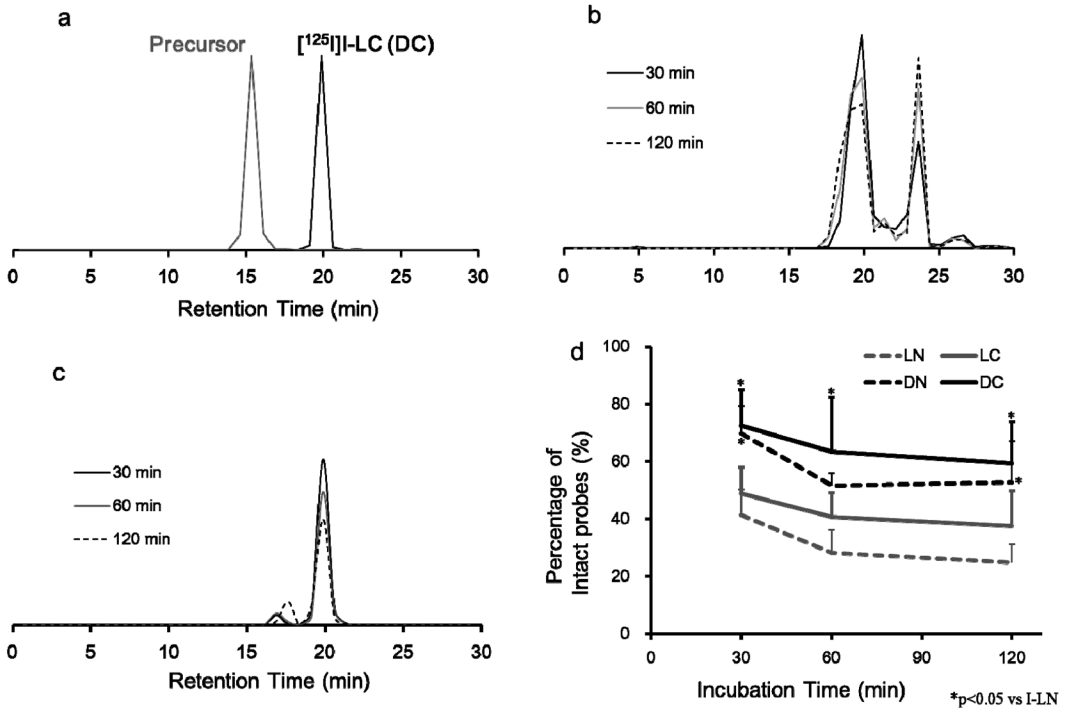

Fig. 2. (a) Representative Chromatograms after Radioiodination

Peaks of precursors (LC or DC) at 15.5 min (gray) detected by UV absorbance (254 nm). Peaks of radioiodinated probes ([123/125]I]I-LC or [123/125]I]I-DC) at 19.2 min (black) detected by RI detector. (b, c) Representative chromatograms of [125]I]I-LC (b) or [125]I]I-DC (c) after incubation with mice plasma. (d) Percentage (mean±S.D.) of intact probes after incubation with mice plasma for 30, 60, and 120 min. *$p<0.05$ *vs.* [125]I]I-LN.

values for [125]I]I-LN, [125]I]I-LC, [125]I]I-DN and [125]I]I-DC of 0.71, 0.42, 0.97, and 0.87 μM, respectively (Table 1). Competitive inhibition studies of I-LN, I-LC, I-DN and I-DC against [125]I]I-LN revealed IC_{50} values of displacement curves to be 1.43, 0.52, 1.76 and 1.02 μM, respectively (Table 1), indicating that all probes would recognize the same site on the MT1-MMP molecule.

Stability Assay in Plasma [125]I]I-DN and [125]I]I-DC tended to be more stable in mouse plasma than did [125]I]I-LN and [125]I]I-LC, which were degraded into hydrophobic fragments (Fig. 2b). The ratios of intact [125]I]I-LN and [125]I]I-LC were 41.4 and 48.8%, respectively, after 30 min incubation in plasma (Fig. 2d). Meanwhile, HPLC analysis showed no considerable degradation of [125]I]I-DN and [125]I]I-DC (Fig. 2c), with ratios of intact [125]I]I-DN and [125]I]I-DC probes being 69.9 and 72.5%, respectively, with 30 min incubation in plasma (Fig. 2d).

***In Vivo* Biodistribution Study** To compare the probes, time radioactivity curves for blood and tumor, with tumor to muscle (T/M) and tumor to blood (T/B) curves as imaging indexes were generated (Fig. 3). [125]I]I-LN and [125]I]I-LC showed rapid blood clearance with 0.98 and 3.72% injected dose (ID)/g 30 min after injection, while [125]I]I-DN and [125]I]I-DC showed relatively high retention in blood with levels of 11.73 and 8.19% ID/g at 30 min (Fig. 3a). Tumor accumulation of [125]I]I-LN and [125]I]I-LC peaked at 2 min (3.80 and 3.27% ID/g) after injection and then sharply decreased, while [125]I]I-DN and [125]I]I-DC accumulation peaked at 10 min (4.60 and 4.79% ID/g) and then slowly decreased (Fig. 3b). Similarly, tumor accumulation and the T/M ratio for [125]I]I-DN and [125]I]I-DC were significantly higher than [125]I]I-LN and [125]I]I-LC at all of the time points tested (Figs. 3b, c). [125]I]I-DC showed the highest T/B ratio after 10 min. (Fig. 3d). Biodistribution data

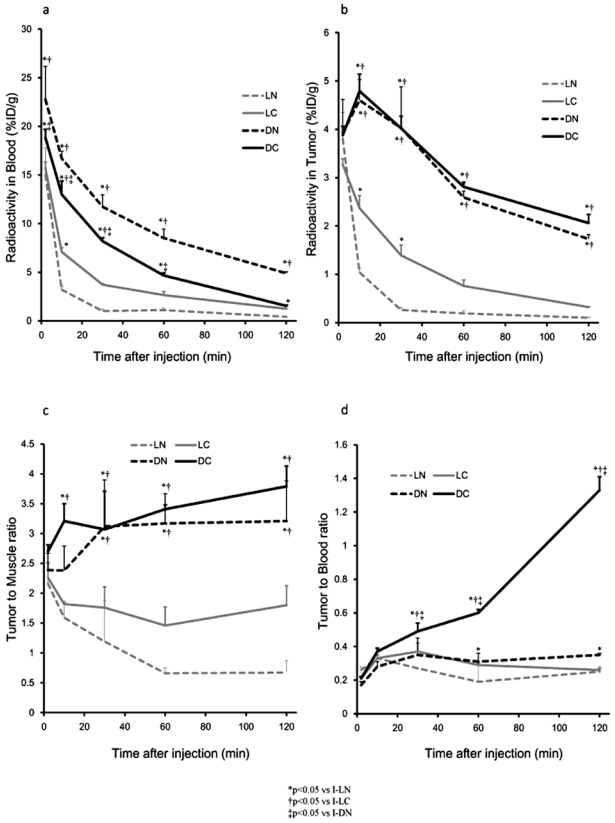

Fig. 3. Radioactivity Accumulation in Blood (a) and Tumor (b) after Injection of Probes, and Tumor to Muscle (c) and Tumor to Blood (d) Ratios of Radioactivity Accumulation of Each Probe at 2, 10, 30, 60 and 120 min after Injection

*$p<0.05$ *vs.* [125]I]I-LN, †$p<0.05$ *vs.* [125]I]I-LC, ‡$p<0.05$ *vs.* [125]I]I-DN.

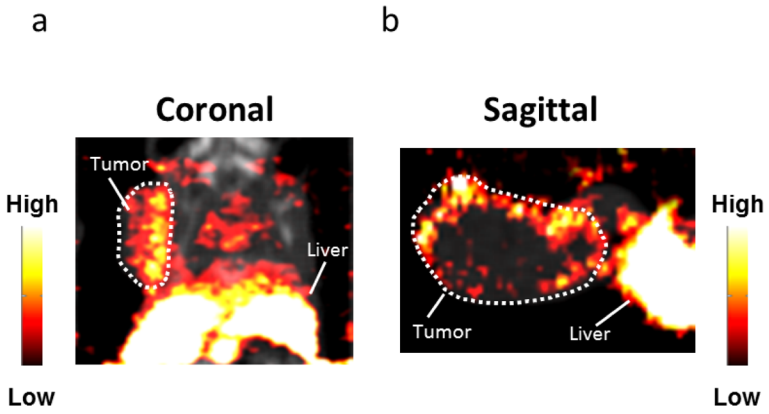

Fig. 4. Coronal (a) and Sagittal (b) Images of a Tumor-Bearing Mouse 30 min after Administration with [^{123}I]I-DC in Focusing on the Thoracic Region as the Field of View

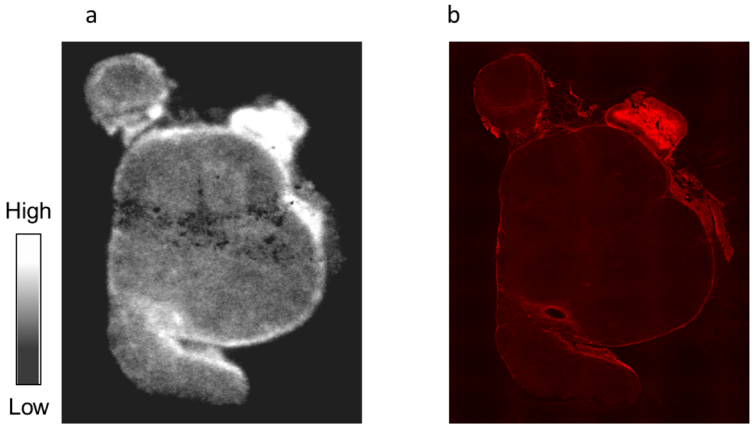

Fig. 5. Representative Images of an Autoradiogram 30 min after Intravenous Administration of [^{123}I]I-DC (a) and MT1-MMP Immunostaining (b)

are described in detail in the Tables ([^{125}I]I-LN, [^{125}I]I-LC and [^{125}I]I-DN and [^{125}I]I-DC in Supplementary Tables S1, S2, S3 and S4, respectively).

SPECT/CT Imaging SPECT/CT was performed using the thoracic region of a tumor-bearing mouse as the field of view 30 min after administration of [^{123}I]I-DC. Coronal and sagittal images (Fig. 4) depicted the subcutaneous implantation of the MT1-MMP-positive tumor on the mouse shoulder and also the liver tissue. The radioactivity tended to be distributed in the marginal regions of the tumor.

***Ex Vivo* Autoradiography and Immunohistochemistry** Similar to the SPECT/CT imaging results, an autoradiogram of a tumor section prepared from tumor tissue excised 30 min after intravenous injection of [^{123}I]I-DC showed that the radioactivity was distributed in the marginal regions of tumor tissue (Fig. 5a). Immunohistochemistry of the adjacent section also indicated the presence of MT1-MMP expression in the marginal regions of the section, and that the radioactivity accumulation profiles tended to correspond to MT1-MMP-positive areas (Fig. 5b).

DISCUSSION

Given earlier findings that MT1-MMP shows various functions and interactions with other molecules in cancer cells,[17] and MT1-MMP is believed to be a useful prognostic factor for cancer malignancy in patients,[18,19] precise *in vivo* evaluation of MT1-MMP expression in cancers can provide beneficial information for both basic and clinical studies.

For this purpose, a newly developed radiolabeled peptide probe, [^{123}I]I-DC, was prepared for imaging MT1-MMP in cancer tissue. [^{123}I]I-DC was easily generated by chemical synthesis as a homogeneous product, and could be successfully radiolabeled with more than 1000-fold higher specific radioactivity than previously reported antibody-derived probes. [^{123}I]I-DC had the capacity to allow the visualization of MT1-MMP-expressing tumors by SPECT (Fig. 4), and the radioactivity distribution profiles corresponding to MT1-MMP-positive areas obtained with this imaging technique were confirmed by *ex vivo* autoradiographic analysis (Fig. 5). These characteristics suggest that [^{123}I]I-DC would thus be a useful probe for *in vivo* MT1-MMP imaging with SPECT and could have the potential for applications in a wide range of cancer research.

To develop these new radiolabeled probes, radioiodinated peptide probes were designed based on a MT1-MMP binding peptide sequence[20] that reportedly recognizes the MT1-MMP amino acid sequence 160–174 (termed the 'MT-loop') located in the catalytic domain, which is thought to be important for activation of proMMP-2.[20,21] This MT-loop sequence is unique to MT1-MMP, which should promote high MT1-MMP specificity of imaging probes that target the MT-loop. In addition, the MT-loop is sterically located on the surface of the MT1-MMP molecule, making this region easily accessible by

drugs, as well as being an appropriate target site for molecular probes.

Many natural peptides, including somatostatin and glucagon-like peptide-1, have proven to be unsuitable for *in vivo* use due to a short plasma half-life. Therefore, to enhance metabolic stability for *in vivo* use, such peptides have been modified in various ways such as incorporation of D-amino acids instead of the original L-amino acids.[22] In this study, we also adopted D-amino acids to make these probes suitable for *in vivo* imaging. Indeed, the D-amino acid-based probes showed significantly higher stability than L-amino acid-based probes, but the D-amino acid probes still reacted with the same binding site on the MT1-MMP molecule with an affinity that was equivalent to L-amino acid-based probes. With regard to the probe labeling position in the peptide sequence that was discussed at the beginning of this study, we first tried to introduce the radiolabeling agent into the amino groups of two lysine residues in the sequence, but this labeling resulted in a significant loss of MT1-MMP binding capacity (described in detail in Supplementary Doc S1, Table S5). Thus, labeling at a cysteine residue added at the N- or C-terminals was used instead to maintain the characteristics of the original peptide.

Among the four probes tested, within 30 min of administration D-amino acid-based probes achieved high tumor retention and a T/M ratio (3–5) that was equivalent to previous antibody-derived probes.[11] In particular, 10 min after injection [^{125}I]I-DC showed significantly faster blood clearance than [^{125}I]I-DN and the highest T/B ratio, which is an important index for *in vivo* imaging (Supplementary Table S4, Fig. 3). Together these results suggest the potential of [^{123}I]I-DC as an *in vivo* imaging probe for MT1-MMP in cancers.

Since MT1-MMP is a promising predictor of the risk for breast cancer recurrence, probes to monitor MT1-MMP expression are needed.[23] For this reason we chose to evaluate the usefulness of [^{123}I]I-DC in SPECT/CT detection of MT1-MMP expression on tumors around the thoracic region. As was expected from the biodistribution data, SPECT successfully delineated the heterogeneous distribution of radioactivity in tumors corresponding to MT1-MMP-positive areas (Figs. 4, 5). We also examined SPECT/CT imaging by administering of [^{123}I]I-DN (Supplementary Fig. S1), but, as was expected from the biodistribution data (Supplementary Table S3), the lung tissues showed high probe accumulation that might be derived from radioactivity in the blood. These characteristics of [^{123}I]I-DN are thought to be unfavorable for clear imaging of cancer. As for [^{123}I]I-LN and [^{123}I]I-LC, we did not perform SPECT/CT imaging in this study because the predicted tumor accumulation of these probes and the T/M ratios revealed by a biodistribution study would be insufficient for imaging cancers. Taken together, these findings indicate that [^{123}I]I-DC could be used for *in vivo* monitoring of MT1-MMP expression. On the other hand, the high radioactivity also seen in the liver was recognized as a major obstacle for reconstructing accurate SPECT images of the thoracic region. Thus, increasing the hydrophilicity of [^{123}I]I-DC to promote radioactivity excretion *via* the kidneys rather than the liver could be a future option to optimize the probe for image improvement.

Some fluorogenic probes that can be activated by or bind to MT1-MMP have been used for successful tumor imaging.[24,25] However, these optical probes were inappropriate for quantitative *in vivo* analysis of MT1-MMP because optical imaging suffers from photon attenuation due to absorption and dispersion as well as autofluorescence. In this regard, nuclear medical imaging would provide more accurate quantitation; therefore, several protein-based radiolabeled probes for MT1-MMP have been developed.[10,11,26] However, such high molecular weight probes have other problems such as probe heterogeneity[13] and low apparent specific radioactivity.[27] In particular, one issue concerning MT1-MMP imaging probes is that the MT1-MMP expression level in cancer was reported to be low (about 1.6×10^5 molecules/HT1080 cell[28]) compared to other tumor markers such as human epidermal growth factor receptor 2 (about 1.6×10^6 molecules/SKOV-3 cell[29]). Therefore, given that imaging of MT1-MMP by nuclear medical techniques using a radiolabeled probe that has low specific radioactivity is difficult because of competitive inhibition on target sites, elevation of the apparent specific radioactivity (reduction of precursor quantity remaining in the final solution) could be a strong strategy for producing useful MT1-MMP imaging probes.[27,29] In this study, the newly developed radioiodinated peptide probes were readily and efficiently obtained as homogeneous probes by site-specific reaction of precursor thiol groups with the maleimide moiety in [$^{123/125}$I]IPM. Furthermore, radioiodinated peptide probes could be completely separated from their precursors by RP-HPLC, so that the probes could be administered with a much higher specific radioactivity (>260 MBq/μg) than was achieved for our previously reported radiolabeled antibody probes (37 kBq/μg).[11] Although [$^{123/125}$I]I-DC showed relatively low affinity for MT1-MMP (K_D=810 nM) compared to our previously developed antibody probes[11] (K_D<40 nM for MT1-MMP) and well-established peptide probes such as RGD peptide probes[30] and ^{90}Y-DOTATOC[31] (K_D<10 nM), the radioactivity distribution profiles nonetheless clearly corresponded to MT1-MMP-positive areas (Fig. 5), likely because of the high specific radioactivity of this probe.

In terms of study limitations, the relatively low tumor accumulation level of [^{125}I]I-DC remains a concern. While the high specific radioactivity of [^{125}I]I-DC successfully compensated for insufficient binding affinity in the *in vivo* study, an enhancement of tumor accumulation levels would be required for further studies. To increase the accumulation of the probes in tumors, an improvement in the probe affinity for MT1-MMP could be a solution. A possible strategy to achieve such enhanced affinity is multimerization, which was used for the RGD peptide that recognizes integrin alphav beta3.[32,33] In fact, we reported that an ^{111}In-labeled diabody, a dimer of scFv, could bind to MT1-MMP in a bivalent manner with higher affinity and increased tumor accumulation compared with scFv.[11] Optimization of labeling could also be an effective strategy because our newly developed [^{123}I]I-DC has a relatively lower MT1-MMP affinity (K_D=810 nM) than the parent peptide (K_D=47.4 nM[14]). Thus it appears that the additional moiety in the DC used for radiolabeling somewhat hindered the interaction between the MT-loop and the peptide sequence. Therefore, insertion of spacer linkers that could impose a separation between the radiolabel group and the peptide may yield probes with higher affinity and enable MT1-MMP to be evaluated more precisely.[34] Nevertheless, this study represents the first report of a radiolabeled peptide probe for imaging of MT1-MMP, and it should be emphasized that the probe was able to detect MT1-MMP *in vivo*.

CONCLUSION

We have developed a novel ^{123}I labeled MT1-MMP imaging peptide probe ([^{123}I]I-DC). [^{123}I]I-DC was readily and economically prepared as a homogeneous probe with much higher specific radioactivity than prior protein-based probes for the visualization of MT1-MMP in cancers. The results of this study suggest that [^{123}I]I-DC may have potential for future applications in MT1-MMP-related research fields and could be a lead compound for further probe optimization.

Acknowledgments This study was supported in part by JSPS KAKENHI Grant Number 22791189 and MEXT KAKENHI Grant Number 23113509. Portions of this study were supported by the New Energy and Industrial Technology Development Organization (NEDO), Japan and an Extramural Collaborative Research Grant of the Cancer Research Institute, Kanazawa University.

Conflict of Interest The authors declare no conflict of interest.

Supplementary Materials The online version of this article contains supplementary materials.

REFERENCES

1) Weigelt B, Peterse JL, van't Veer LJ. Breast cancer metastasis: markers and models. *Nat. Rev. Cancer*, **5**, 591–602 (2005).
2) Yamaguchi H, Wyckoff J, Condeelis J. Cell migration in tumors. *Curr. Opin. Cell Biol.*, **17**, 559–564 (2005).
3) Page-McCaw A, Ewald AJ, Werb Z. Matrix metalloproteinases and the regulation of tissue remodelling. *Nat. Rev. Mol. Cell Biol.*, **8**, 221–233 (2007).
4) Jones JL, Glynn P, Walker RA. Expression of MMP-2 and MMP-9, their inhibitors, and the activator MT1-MMP in primary breast carcinomas. *J. Pathol.*, **189**, 161–168 (1999).
5) Ohuchi E, Imai K, Fujii Y, Sato H, Seiki M, Okada Y. Membrane type 1 matrix metalloproteinase digests interstitial collagens and other extracellular matrix macromolecules. *J. Biol. Chem.*, **272**, 2446–2451 (1997).
6) Knäuper V, Will H, López-Otin C, Smith B, Atkinson SJ, Stanton H, Hembry RM, Murphy G. Cellular mechanisms for human procollagenase-3 (MMP-13) activation. Evidence that MT1-MMP (MMP-14) and gelatinase a (MMP-2) are able to generate active enzyme. *J. Biol. Chem.*, **271**, 17124–17131 (1996).
7) Itoh Y, Seiki M. MT1-MMP: a potent modifier of pericellular microenvironment. *J. Cell. Physiol.*, **206**, 1–8 (2006).
8) Brinckerhoff CE, Matrisian LM. Matrix metalloproteinases: a tail of a frog that became a prince. *Nat. Rev. Mol. Cell Biol.*, **3**, 207–214 (2002).
9) Crispi S, Calogero RA, Santini M, Mellone P, Vincenzi B, Citro G, Vicidomini G, Fasano S, Meccariello R, Cobellis G, Menegozzo S, Pierantoni R, Facciolo F, Baldi A, Menegozzo M. Global gene expression profiling of human pleural mesotheliomas: identification of matrix metalloproteinase 14 (MMP-14) as potential tumour target. *PLoS ONE*, **4**, e7016 (2009).
10) Temma T, Sano K, Kuge Y, Kamihashi J, Takai N, Ogawa Y, Saji H. Development of a radiolabeled probe for detecting membrane type-1 matrix metalloproteinase on malignant tumors. *Biol. Pharm. Bull.*, **32**, 1272–1277 (2009).
11) Kondo N, Temma T, Shimizu Y, Watanabe H, Higano K, Takagi Y, Ono M, Saji H. Miniaturized antibodies for imaging membrane type-1 matrix metalloproteinase in cancers. *Cancer Sci.*, **104**, 495–501 (2013).
12) Kenanova V, Wu AM. Tailoring antibodies for radionuclide delivery. *Expert Opin. Drug Deliv.*, **3**, 53–70 (2006).
13) Schumacher FF, Sanchania VA, Tolner B, Wright ZV, Ryan CP, Smith ME, Ward JM, Caddick S, Kay CW, Aeppli G, Chester KA, Baker JR. Homogeneous antibody fragment conjugation by disulfide bridging introduces 'spinostics.' *Sci. Rep.*, **3**, 1525 (2013).
14) Zhu L, Wang H, Wang L, Wang Y, Jiang K, Li C, Ma Q, Gao S, Wang L, Li W, Cai M, Wang H, Niu G, Lee S, Yang W, Fang X, Chen X. High-affinity peptide against MT1-MMP for *in vivo* tumor imaging. *J. Control. Release*, **150**, 248–255 (2011).
15) Luo Z, Zhang S. Designer nanomaterials using chiral self-assembling peptide systems and their emerging benefit for society. *Chem. Soc. Rev.*, **41**, 4736–4754 (2012).
16) Khawli LA, van den Abbeele AD, Kassis AI. *N*-(*m*-[125I]Iodophenyl)maleimide: an agent for high yield radiolabeling of antibodies. *Int. J. Rad. Appl. Instrum. B*, **19**, 289–295 (1992).
17) Gonzalo P, Moreno V, Gálvez BG, Arroyo AG. MT1-MMP and integrins: Hand-to-hand in cell communication. *Biofactors*, **36**, 248–254 (2010).
18) Peng CW, Wang LW, Fang M, Yang GF, Li Y, Pang DW. Combined features based on MT1-MMP expression, CD11b + immunocytes density and LNR predict clinical outcomes of gastric cancer. *J. Transl. Med.*, **11**, 153 (2013).
19) He L, Chu D, Li X, Zheng J, Liu S, Li J, Zhao Q, Ji G. Matrix metalloproteinase-14 is a negative prognostic marker for patients with gastric cancer. *Dig. Dis. Sci.*, **58**, 1264–1270 (2013).
20) Fernandez-Catalan C, Bode W, Huber R, Turk D, Calvete JJ, Lichte A, Tschesche H, Maskos K. Crystal structure of the complex formed by the membrane type 1-matrix metalloproteinase with the tissue inhibitor of metalloproteinases-2, the soluble progelatinase A receptor. *EMBO J.*, **17**, 5238–5248 (1998).
21) English WR, Holtz B, Vogt G, Knäuper V, Murphy G. Characterization of the role of the "MT-loop": an eight-amino acid insertion specific to progelatinase A (MMP2) activating membrane-type matrix metalloproteinases. *J. Biol. Chem.*, **276**, 42018–42026 (2001).
22) Fani M, Maecke HR. Radiopharmaceutical development of radiolabelled peptides. *Eur. J. Nucl. Med. Mol. Imaging*, **39** (Suppl. 1), S11–S30 (2012).
23) Ogura S, Ohdaira T, Hozumi Y, Omoto Y, Nagai H. Metastasis-related factors expressed in pT1 pN0 breast cancer: assessment of recurrence risk. *J. Surg. Oncol.*, **96**, 46–53 (2007).
24) Shimizu Y, Temma T, Sano K, Ono M, Saji H. Development of membrane type-1 matrix metalloproteinase-specific activatable fluorescent probe for malignant tumor detection. *Cancer Sci.*, **102**, 1897–1903 (2011).
25) Zhu L, Zhang F, Ma Y, Liu G, Kim K, Fang X, Lee S, Chen X. *In vivo* optical imaging of membrane-type matrix metalloproteinase (MT-MMP) activity. *Mol. Pharm.*, **8**, 2331–2338 (2011).
26) Van Steenkiste M, Oltenfreiter R, Frankenne F, Vervoort L, Maquoi E, Noel A, Foidart JM, Van De Wiele C, De Vos F. Membrane type 1 matrix metalloproteinase detection in tumors, using the iodinated endogenous [^{123}I]-tissue inhibitor 2 of metalloproteinases as imaging agent. *Cancer Biother. Radiopharm.*, **25**, 511–520 (2010).
27) Tolmachev V, Wållberg H, Sandström M, Hansson M, Wennborg A, Orlova A. Optimal specific radioactivity of anti-HER2 Affibody molecules enables discrimination between xenografts with high and low HER2 expression levels. *Eur. J. Nucl. Med. Mol. Imaging*, **38**, 531–539 (2011).
28) Zucker S, Hymowitz M, Conner CE, DiYanni EA, Cao J. Rapid trafficking of membrane type 1-matrix metalloproteinase to the cell surface regulates progelatinase A activation. *Lab. Invest.*, **82**, 1673–1684 (2002).
29) Tolmachev V, Tran TA, Rosik D, Sjöberg A, Abrahmsén L, Orlova A. Tumor targeting using affibody molecules: interplay of affinity, target expression level, and binding site composition. *J. Nucl. Med.*,

53, 953–960 (2012).
30) Ueda M, Fukushima T, Ogawa K, Kimura H, Ono M, Yamaguchi T, Ikehara Y, Saji H. Synthesis and evaluation of a radioiodinated peptide probe targeting $\alpha v\beta 6$ integrin for the detection of pancreatic ductal adenocarcinoma. *Biochem. Biophys. Res. Commun.*, **445**, 661–666 (2014).
31) Waldherr C, Pless M, Maecke HR, Haldemann A, Mueller-Brand J. The clinical value of [90Y-DOTA]-D-Phe1-Tyr3-octreotide (90Y-DOTATOC) in the treatment of neuroendocrine tumours: a clinical phase II study. *Ann. Oncol.*, **12**, 941–945 (2001).
32) Dijkgraaf I, Yim CB, Franssen GM, Schuit RC, Luurtsema G, Liu S, Oyen WJ, Boerman OC. PET imaging of $\alpha v\beta_3$ integrin expression in tumours with ^{68}Ga-labelled mono-, di- and tetrameric RGD peptides. *Eur. J. Nucl. Med. Mol. Imaging*, **38**, 128–137 (2011).
33) Dijkgraaf I, Kruijtzer JA, Liu S, Soede AC, Oyen WJ, Corstens FH, Liskamp RM, Boerman OC. Improved targeting of the alpha(v)beta (3) integrin by multimerisation of RGD peptides. *Eur. J. Nucl. Med. Mol. Imaging*, **34**, 267–273 (2007).
34) Fragogeorgi EA, Zikos C, Gourni E, Bouziotis P, Paravatou-Petsotas M, Loudos G, Mitsokapas N, Xanthopoulos S, Mavri-Vavayanni M, Livaniou E, Varvarigou AD, Archimandritis SC. Spacer site modifications for the improvement of the *in vitro* and *in vivo* binding properties of (99m)Tc-N(3)S-X-bombesin[2–14] derivatives. *Bioconjug. Chem.*, **20**, 856–867 (2009).